Sensors and Actuators B 259 (2018) 587–595

Contents lists available at ScienceDirect

Sensors and Actuators B: Chemical

journal homepage: www.elsevier.com/locate/snb

Microfluidic diatomite analytical devices for illicit drug sensing with ppb-Level sensitivity

Xianming Kong[a,b], Xinyuan Chong[b], Kenny Squire[b], Alan X. Wang[b,*]

[a] College of Chemistry, Chemical Engineering and Environment Engineering, Liaoning Shihua University, Fushun, Liaoning, 113001, PR China
[b] School of Electrical Engineering and Computer Science, Oregon State University, Corvallis, OR, 97331, USA

ARTICLE INFO

Article history:
Received 10 October 2017
Received in revised form 5 December 2017
Accepted 7 December 2017
Available online 16 December 2017

Keywords:
Drug detection
Microfluidic device
Photonic crystals
Point-of-care
Lab-on-a-chip

ABSTRACT

The escalating research interests in porous media microfluidics, such as microfluidic paper-based analytical devices, have fostered a new spectrum of biomedical devices for point-of-care (POC) diagnosis and biosensing. In this paper, we report microfluidic diatomite analytical devices (μDADs), which consist of highly porous photonic crystal biosilica channels, as an innovative lab-on-a-chip platform to detect illicit drugs. The μDADs in this work are fabricated by spin-coating and tape-stripping diatomaceous earth on regular glass slides with cross section of $400 \times 30\ \mu m^2$. As the most unique feature, our μDADs can simultaneously perform on-chip chromatography to separate small molecules from complex biofluidic samples and acquire the surface-enhanced Raman scattering spectra of the target chemicals with high specificity. Owing to the ultra-small dimension of the diatomite microfluidic channels and the photonic crystal effect from the fossilized diatom frustules, we demonstrate unprecedented sensitivity down to part-per-billion (ppb) level when detecting pyrene (1ppb) from mixed sample with Raman dye and cocaine (10 ppb) from human plasma. This pioneering work proves the exclusive advantage of μDADs as emerging microfluidic devices for chemical and biomedical sensing, especially for POC drug screening.

1. Introduction

In recent years, the escalation of research interests in porous media microfluidics [1,2], especially microfluidic paper-based analytical devices (μPADs) [3–5], have fostered a new spectrum of biomedical devices for point-of-care diagnosis and biosensing. μPADs can be fabricated by simple, low-cost processes using conventional photo- or soft lithographic techniques, utilizing either photoresists [6] or wax printing [7]. Advantages of using μPADs for microfluidic channels include: 1) ubiquitous and extremely cheap cellulosic materials; 2) capillary flow which enables fluid transport without using any external pump; and 3) compatible with many chemical and biomedical applications. Many different chemical and biological assays have been performed using μPADs, including for the detection of glucose [8], protein (albumin) [9], cholesterol [10], and heavy metals [11]. They have also been used as platforms for ELISA [12]. Especially, I. M. White's group used inkjet-printed paper-based surface-enhanced Raman scattering (SERS) substrates for chromatographic separation and detection of target analytes from complex samples [13], which opened a new route for on-chip chemical sensing.

Other than μPADs, porous silica materials and devices also have attracted considerable attention for biosensing due to the use of their large surface area and pore volume to achieve high sensitivity [14,15]. The high porosity, which allows for the immobilization of target molecules not only on the external surface of the substrate but also inside of the pores, enables the loading of large amounts of sensing molecules, giving instant responses and high sensitivity. The optical transparency, on the other hand, permits optical detection through the bulk of the material. In addition, the surface groups and biocompatibility also makes porous silica one of the most potential materials for biosensing. Moon et al. have fabricated polymer and colloidal silica porous composite for nucleic acid biosensing [16]. Yang et al. have synthesized porous SiO_2 material and used it as enzyme immobilization carriers to fabricate glucose biosensors [17]. However, the pores in sol–gel derived silica lack a high degree of order, which results in random paths and consequently non-uniform diffusion of the analytes. A fraction of the sensing molecules might even be unreachable, leading to low response and poor spatial resolution [18].

Diatoms are unicellular, photosynthetic, bio-mineralized marine organisms that possess a biosilica shell, which is called the frustule. The two-dimensional (2-D) periodic pores on diatom

* Corresponding author.
E-mail address: wang@eecs.oregonstate.edu (A.X. Wang).

https://doi.org/10.1016/j.snb.2017.12.038
0925-4005/

surface enable it unique optical, physical, and chemical properties [19,20]. In recent decades, a variety of biosensors with ultra-high sensitivity using diatom biosilica have been reported [21]. Zhen et al. developed photoluminescence-based diatom biosensors that have been successfully applied for 2, 4, 6-trinitrotoluene (TNT) sensing [22]. De Stefano et al. have fabricated highly-selective biosensor for immuno-complex detection by modifying diatom frustules (*Coscinodiscus concinnus*) with antibodies [23]. From the optics perspective, the photonic crystal feature of diatoms could provide additional SERS enhancement when hybridized with plasmonic nanostructures [24,25]. Our group has developed an in-situ growth method for depositing silver nanoparticles (Ag NPs) on diatom for ultrasensitive, label-free TNT sensing [26,27]. Other than natural photonic crystal structures from living diatoms, diatomite consists of fossilized remains of ancient diatoms as geological deposits with billions of tons of reserve on earth. Therefore, diatomite is a type of naturally abundant photonic crystal biosilica, which has been widely used in industry as water filters, adsorbents, and medicine [28–30]. Diatomite has similar properties to diatoms such as highly porous structure, excellent adsorption capacity, and photonic crystal effects [31,32].

In this study, we report microfluidic diatomite analytical devices (μDADs), which consist of nano-porous photonic crystal biosilica channels for label-free biosensing of illicit drugs from complex biological samples using on-chip chromatography in conjunction with SERS sensing method. Previously, bio-inspired photonic crystals have been integrated into microfluidic systems as lab-on-a-chip system [33] and SERS has been employed for drug sensing [34]. In this research, Cocaine ($C_{17}H_{21}NO_4$) is chosen as the target analyte in our study, which is an alkaloid derived from coca leaves. Cocaine is one of the most widely used illicit drugs all over the world according to the latest World Drug Report from the United Nations Office on Drugs and Crime (UNODC). Cocaine is a potent stimulant of the central nervous system that leads to a state of increased alertness and euphoria. Its effect is similar to that of amphetamines but with shorter duration. In this study, we report using μDADs for on-chip chromatography-SERS to separate and detect cocaine from real biofluidic samples. The μDADs achieve nearly 1000 times better limit of detection (LOD) than normal chromatography plates to 1–10 ppb level, which is comparable or even higher than that of many laboratory analysis techniques [35], which will be discussed in Section 3.6.

2. Materials and methods

2.1. Materials and reagents

Tetrachloroauric acid ($HAuCl_4$) was purchased from Alfa Aesar (USA). Trisodium citrate ($Na_3C_6H_5O_7$), anhydrous ethanol, hexane and ethyl acetate were purchased from Macron (USA). Celite209 (diatomite), carboxymethyl cellulose, pyrene, 4-mercaptobenzoic acid (MBA), plasma and cocaine were obtained from Sigma-Aldrich(USA). The chemical reagents used were of analytical grade. Water used in all experiments was deionized and further purified by a Millipore Synergy UV Unit (Millipore-Sigma USA) to a resistivity of ~18.2 MΩ cm.

2.2. Preparation and characterization of gold nanoparticles (Au NPs)

The glassware used through the NP synthesis process was cleaned with aqua regia (HNO_3/HCl, 1:3, v/v) followed by rinsing thoroughly with Milli-Q water. Au NPs with an average diameter of 60 nm were prepared using sodium citrate as the reducing and stabilizing agent according to the literature with little modification [36]. Briefly, a total of 100 mL of 1 mM chloroauric acid aqueous solution was heated to boiling under vigorous stirring. After adding 4.1 mL of 1% trisodium citrate, the pale yellow solution turned fuchsia within several minutes. The colloids were kept under reflux for another 15 min to ensure complete reduction of Au^{3+} ions followed by cooling to room temperature. For practical point-of-care (POC) sensing, the Au NPs will be concentrated by centrifuge and stored in refrigerators with expected life time of more than 1 month.

2.3. Fabrication of μDADs

The diatomaceous earth substrates were fabricated by spin coating diatomite on glass slides. The diatomite was dried at 150 °C for 6 h in an oven before spin-coating the glass slides. After cooling to room temperature, 11.55 g of diatomite was first dispersed in 20 mL of 0.4% aqueous solution of carboxymethyl cellulose and then deposited onto the glass slide by spin-coating at 1300 rpm for 20 s. The porous photonic crystal biosilica channels were fabricated by a simple tape-stripping method as shown in Fig. S1: the glass slides were first covered by an adhesive tape; then 400 μm wide channel array was cut by a razor blade through the tape; after spin-coating with diatomite, the tape was removed gently, leaving 400 × 30 μm^2 cross section diatomite channel array on the glass substrate. Last, the μDADs were dried in shade and activated at 110 °C for 3 h to improve the adhesion of diatomite to the glass slide.

2.4. μDADs for on-chip chromatography-SERS biosensing

The on-chip chromatography-SERS sensing method was designed for ultra-sensitive detection of analytes from mixtures or complex biofluid as shown in Scheme 1. First, 0.2 μL liquid sample was spotted onto the reservoir (circular region) of the μDAD. After drying in air, the bottom tips of the μDADs were immersed in the solvent which migrates along the porous channels towards the other end of the μDADs due to capillary forces. After that, the μDADs were taken out from the solvent and dried in air. The separated analyte spots along the porous channels were marked under ultraviolet illumination at 380 nm wavelength and visualized by iodine colorimetry. Then 2 μL of concentrated Au NPs in solution were dropped onto the corresponding spots directly. An alternative method to avoid dispensing the colloid solution is to pre-deposit Au NPs using inkjet printer at the designated spots. However, this process requires precise calibration of the analyte migration rate and will be investigated in our future research. A Horiba Jobin Yvon(USA) Lab Ram HR800 Raman microscope equipped with a CCD detector (uEye cmos, Germany) was used to acquire the Raman spectra, and a 50× objective lens (Olympus Mplan, Japan) was used to focus the laser onto the SERS substrates. A 785 nm laser was chosen as the excitation wavelength and the laser spot size was 2 μm in diameter. The confocal pinhole was set to a diameter of 200 μm. The acquired data was processed with Horiba LabSpec 5 software. Fluorescence spectra were acquired using the previous method [37]. Briefly, we focus light to a diatom surface with the 50× objective lens using the Horiba Jobin Yvon Lab Ram HR800 Raman system with 325 nm UV line.

2.5. Other instruments

UV-vis absorption spectra were recorded on NanoDrop 2000 UV–vis spectrophotometer (Thermo Scientific USA) using quartz cells of 1 cm optical path. Scanning electron microscopy (SEM) images were acquired on FEI Quanta 600 FEG SEM (Thermo Scientific, USA) with 15–30 kV accelerating voltage. The microscopy images were obtained using Olympus (Japan) IX73 microscope with 20× objective lens.

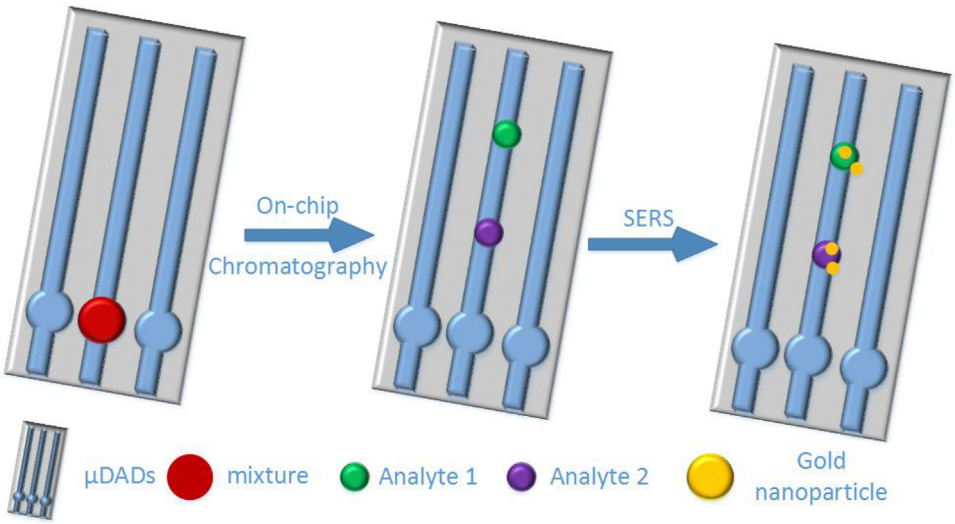

Scheme 1. Schematic illustration of on-chip chromatography-SERS biosensing using the proposed μDADs.

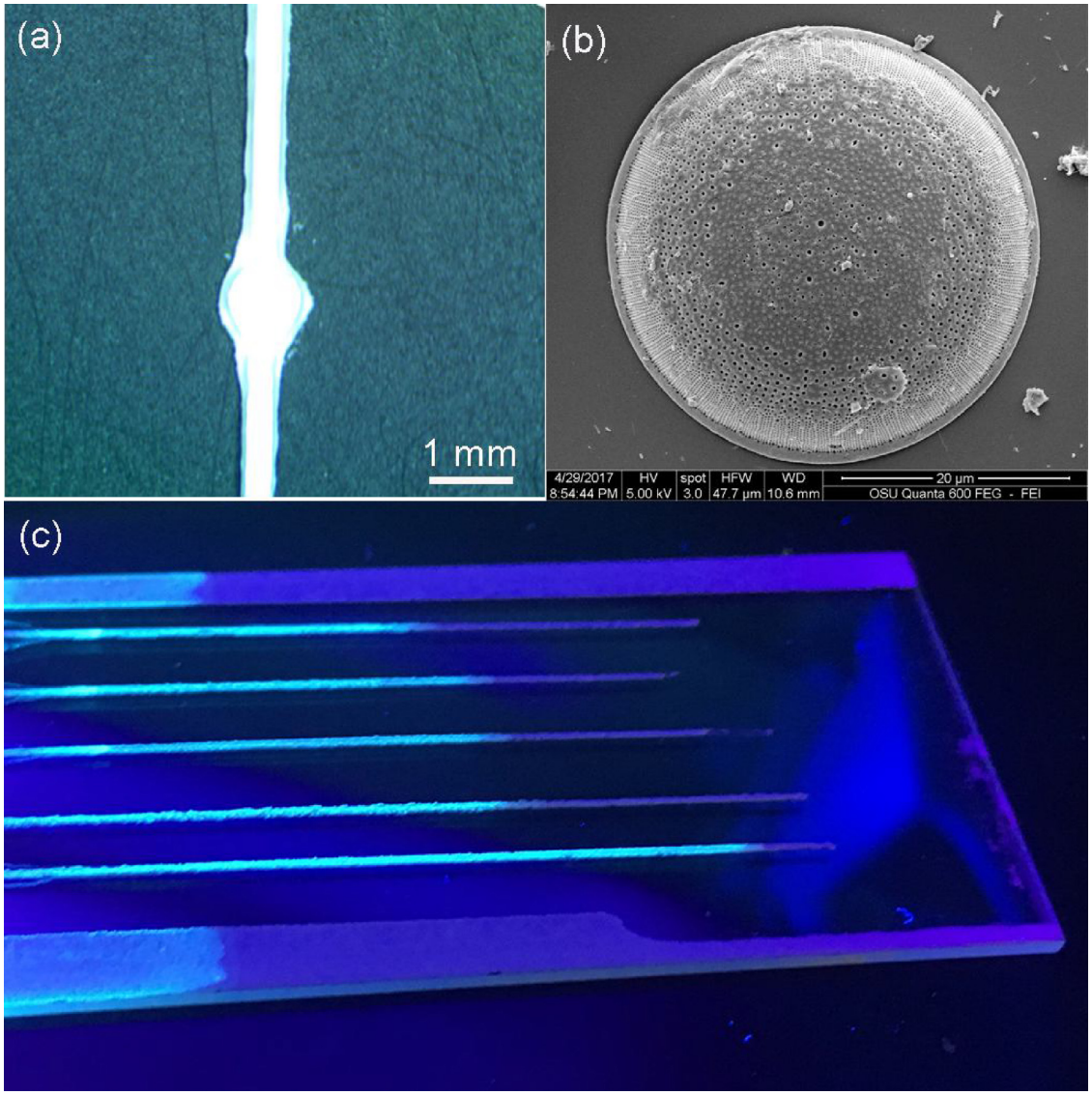

Fig. 1. Optical image of the μDADs (a) and SEM image of the honeycomb-like diatomite (b), which forms the micro-channels of μDADs, and optical image of μDADs after 100 ppm pyrene migration illuminated by UV light (c).

3. Results and discussion

3.1. Synthesis of Au colloid

SEM and UV–vis absorption spectroscopy were employed to characterize the quality of the prepared Au NPs. The SEM image (Fig. S2) indicates that the Au NPs have a spherical shape with uniform size distribution and their diameters are estimated to be 50–60 nm. The UV–vis spectra of Au colloids were shown in Fig. S3. The wavelength and intensity of the maximum absorption of the plasmonic NPs depends on the size, shape, concentration and surrounding dielectric environment around the nanoparticles. The localized surface plasmon resonance (LSPR) peak of the prepared Au colloids is located at 549 nm. These values correspond to relatively uniform, mono-dispersed Au colloids with diameters of approximately 50–60 nm.

3.2. Micro- & nano-structures of the μDADs

The morphology of μDADs was characterized by SEM as shown Fig. 1(a). The width of the porous diatomite channels was nearly 400 μm. The reservoir (circular region) with diameter of 1 mm was used for sample dispensing. The porous diatomite channels mainly consist of disk-shaped diatomite biosilica. The morphology of the diatomite biosilica was shown in Fig. 1(b) and the 2D periodic pores with sub-micron diameters on diatomite enables guided-mode resonances (GMRs) of photonic crystals[38], which has similar effect to diatom biosilica as we have reported previously [26]. In order to verify the photonic crystal effect of diatomite, the near field optical microscopic image of a single diatomite is shown in Fig. S4. The light pattern comes from the high order diffraction of the photonic crystals, which agrees with the results from Stefano's group. [39]. Therefore, the nanostructures of diatomite provide photonic crystal effects, although it may not be perfect. The highly porous structure and uniform pore size of diatomite divide the stationary phase into smaller entities, thus decreasing the length of each diffusional segment paths [40], which enables more homogenous fluid flows into the pores of diatomite. Therefore, the eluent flows more smoothly and uniformly along μDADs due to capillary forces without any external pump. In order to verify the fluid flow within the porous photonic crystal biosilica channels, 100 ppm pyrene solution was used as the fluidic sample. After fluid flowing, the porous photonic crystal biosilica channels were illuminated by UV light as shown in Fig. 1(c). The fluorescence color from pyrene was observed in contrast to the glass substrate, which indicated that the 3D μDADs porous structure enabled pump-free fluid flow successfully.

3.3. On-chip chromatography using the μDADs

Polychromatic hydrocarbons (PAHs) are a class of aromatic compounds consisting of two or more aromatic or heterocyclic rings. The detection of various PAHs has significant engineering potential as PAHs are harmful to the environment and public health. Unfortunately, the low binding affinity between PAHs and the surface of metallic substrates prevents efficient SERS detection of PAHs from mixtures as the spectra from co-existing components interfere with the SERS spectra from the PAHs [41]. We first investigated the potential of using SERS to detect MBA, Pyrene and their mixture. Fig. 2(a) shows the SERS spectra of MBA, pyrene and their mixture. MBA is a commonly used Raman probe molecule because of its strong binding affinity with metallic surfaces and intense Raman signals. The peaks located at 1074 and 1587 cm^{-1} are associated with the C—C ring-breathing modes of MBA [42]. For mixture (Pyrene: MBA = 1:1) solution, the metallic surface coverage was dominated by MBA because covalent bonds can be formed easily between the Au NPs and the mercapto group of MBA. Thus only a very weak Raman peak from pyrene was observed from the SERS spectra of the mixture. It is difficult to distinguish the Raman peak of pyrene from the mixture by normal SERS without separating MBA.

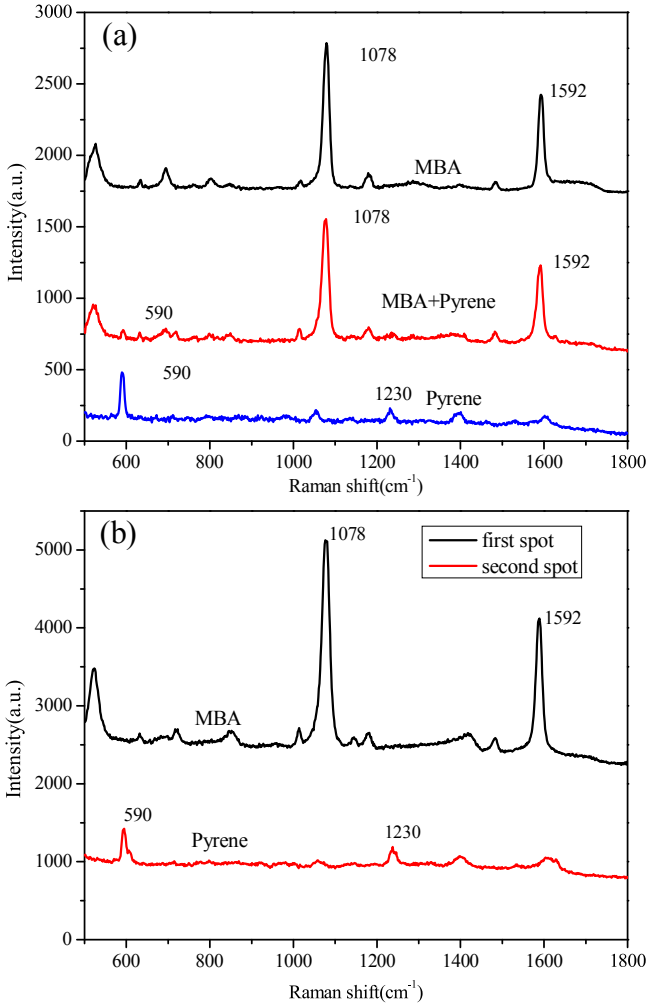

Fig. 2. (a) SERS spectra of pure substance of MBA, pyrene and the mixture; and (b) SERS spectra of different spots on μDADs after chromatography separation.

When the fluid flows along the μDADs via the capillary force, the diatomite functions as the stationary phase for chromatography because the abundance of hydroxyl groups on diatomite surfaces make it highly polar. After the mixture sample has been dropped to the reservoirs of μDADs, the organic eluent flows along the channels. More polar compound molecules will have stronger interaction with the diatomite and will migrate at a slower speed. We first investigated the separation effect of μDADs with pyrene and MBA mixture. Hexane and ethyl acetate (v/v = 6:1) were used as the eluent for the separation of pyrene from the mixture. After complete fluid flow, a UV lamp and iodine colorimetry was used to visualize different analyte spots corresponding to pyrene and MBA. Pyrene migrated faster and was located further from the original dropping point at the reservoir because the lower molecular polarity induces weaker affinity with polar diatomite surface. The SERS spectra at corresponding spots were collected on the surface of μDADs as shown in Fig. 2(b). The characteristic peaks of pyrene at 590 cm^{-1} and 1230 cm^{-1} are clearly observed, which means that the μDADs can successfully be used as the stationary phase for on-chip chromatography.

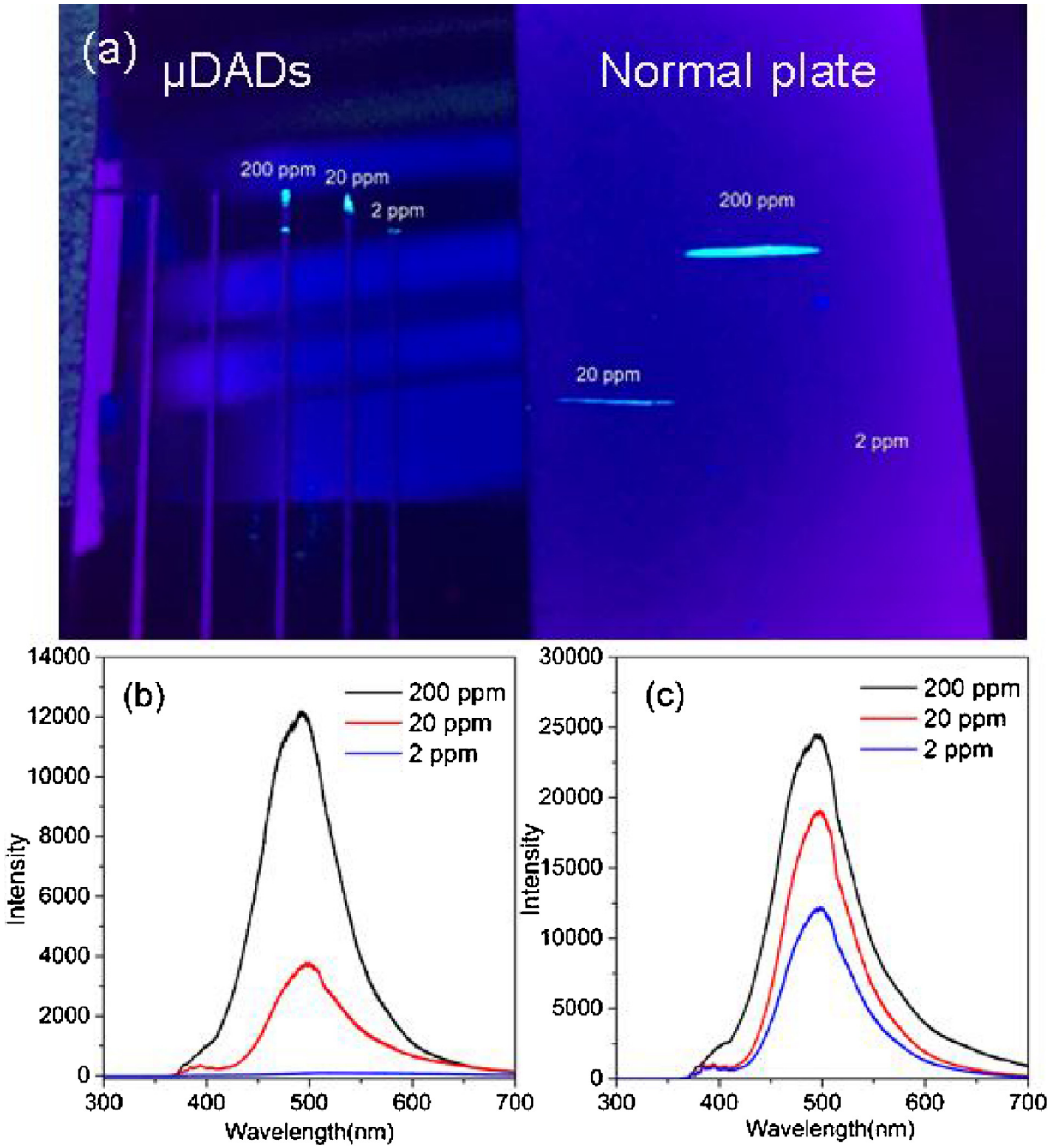

Fig. 3. (a) Photographic images of different concentrations of pyrene separated by μDADs and normal diatomite plates. The spots after separation are visualized by UV light; fluorescence spectra of different concentrations of pyrene separated by normal diatomite chromatography plates (b) and μDADs (c).

3.4. Confinement of the analyte by μDADs

In general, the intensity of SERS signals $I_{SERS(vs)}$ can be estimated as [43,44]:

$$I_{SERS}(V_S) \propto N_M \times |A(V_L)|^2 \times |A(V_S)|^2 \times \delta^R_{ads}$$

where N_M is the number of molecules involved in the SERS measurement, δ^R_{ads} is the Raman cross section of the molecule that is being detected, and $A(V_L)$ and $A(V_S)$ are the electrical field enhancement factors at the excitation laser and Stokes frequency for the Raman signal enhancement. These parameters usually are intrinsic factors which are nearly constant for the same SERS substrate and the target molecules other than N_M [44]. In most on-chip chromatography SERS devices, the plasmonic nanoparticles are dispensed onto the analyte spots after chromatography separation. The SERS spectra collected from each spot will only come from the target molecules at the surface of the chromatography chip. This means that the overall SERS intensity will be dependent on the amount of target molecules in close proximity to the plasmonic NPs at the surface of the chromatography plate. We have reported previously that thinner diatomite layers will effectively concentrate the analyte at the surface of the chromatography plate [45]. Compared with thin film plate, the μDADs we fabricated can confine the liquid flow within a $400 \times 30\ \mu m^2$ cross section channel, which significantly enhances the target molecule concentration at the surface of μDADs.

The confinement of the analyte molecules by μDADs was investigated by fluorescence microscopy and spectra. First, 0.2 μL and

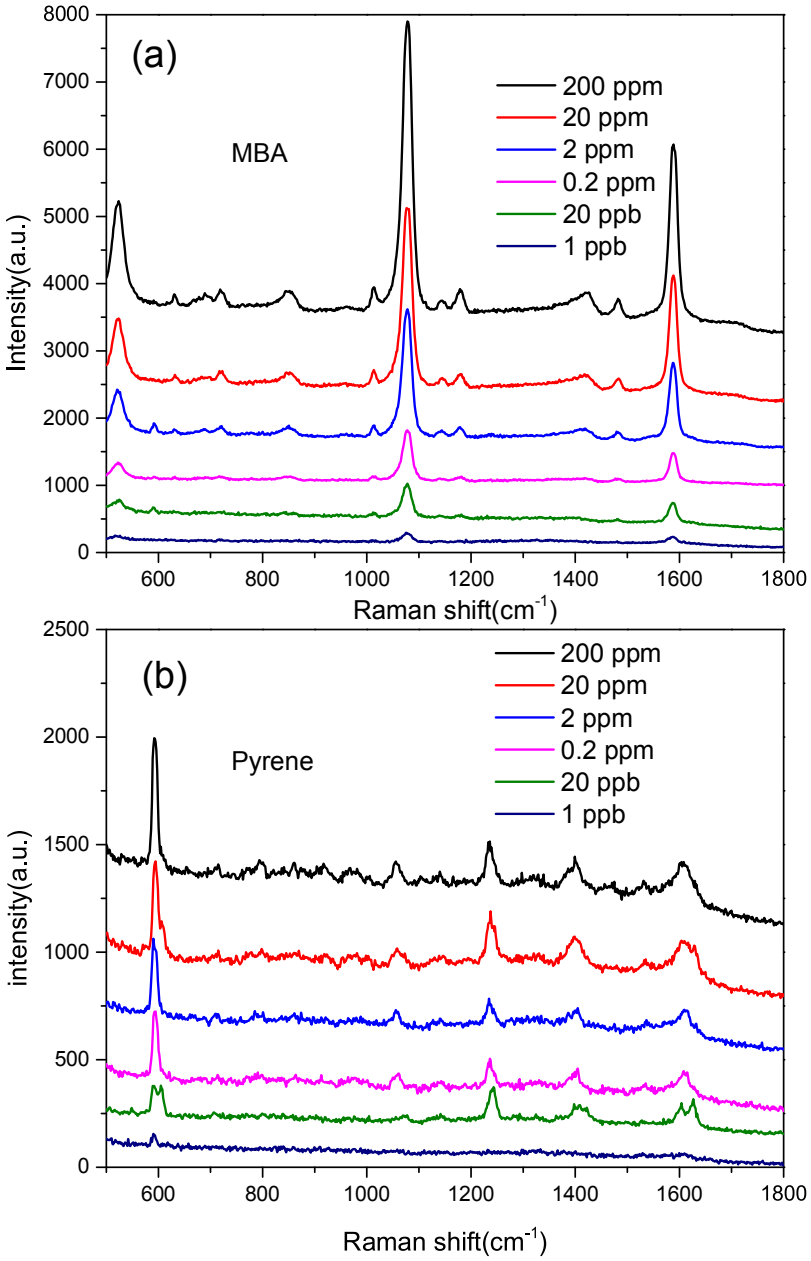

Fig. 4. SERS spectra of MBA on the first spot (a) and pyrene on the second spot (b) from mixture (pyrene: MBA = 1:1) at different concentrations separated by μDADs.

1 μL of pyrene solution with 200 ppm, 20 ppm and 2 ppm concentrations was dispensed onto the μDADs and normal diatomite chromatography plate respectively. After eluent migrating, the substrate was illuminated by a UV laser, as shown in Fig. 3(a). From the optical images, we can observe fluorescence spots on the two chips. For 20 ppm concentration of pyrene, the fluorescence spot from μDADs chip is brighter than that from normal chromatography plate. With the concentration of pyrene down to 2 ppm, fluorescence spot on μDADs was still obvious while there was no observable fluorescence spot from the normal chromatography plate.

Such confinement effect to target molecules was also confirmed by fluorescence spectra as shown in Fig. 3. The samples used to acquire the fluorescence spectra were the same as those for the fluorescence images. In Fig. 3(b), the intensity of fluorescence spectra of pyrene decreases with reduced pyrene concentration. When the concentration of pyrene is 2 ppm, only weak fluorescence spectra of pyrene were observed. As shown in Fig. 3(c), the fluorescence spectra of pyrene from μDADs at the spot of 2 ppm pyrene still showed intense fluorescence signals. In principle, the number of pyrene molecules on the normal chromatography chip (1 μL) should be higher that spotted onto μDADs (0.2 μL), but the intensity of the fluorescence spectra was in the opposite manner. A smaller amount of pyrene in the μDADs shows higher fluorescence intensity than that from 20 ppm pyrene on normal chromatography chip, therefore it proves that narrow micro-channels have stronger confinement effect of target molecules.

3.5. Ultrasensitive on-chip sensing of pyrene from mixture by μDADs

The μDADs were employed for sensing pyrene from mixture. We compared the SERS spectra obtained from the μDADs as shown in Fig. 4(a) and (b) with normal diatomite chromatography chip (Fig. S5). In Fig. 4, all the characteristic bands of MBA and pyrene exhibited monotonous decrease in intensity as the mixture concen-

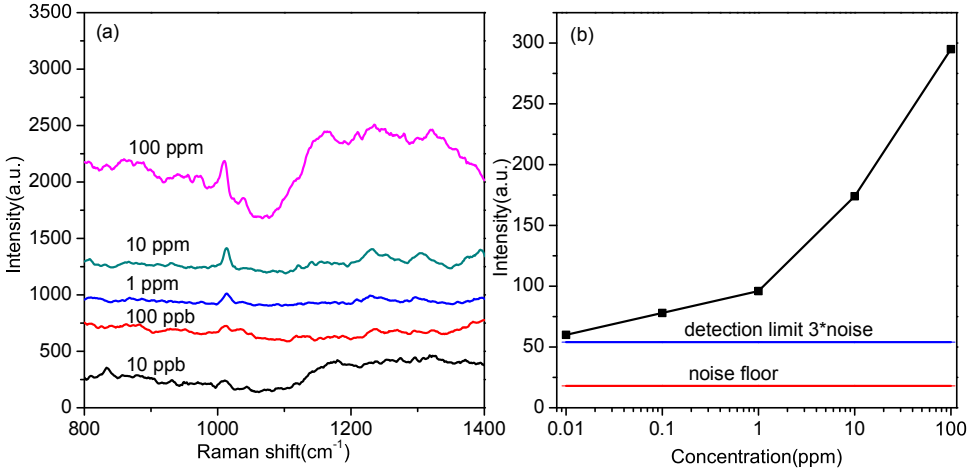

Fig. 5. SERS spectra of human plasma with different concentrations of cocaine separated by μDADs (a) and the SERS intensity as a function of logarithm scale Cocaine concentration in Plasma (b). The detection limit was indicated as the line in (b).

tration decreases. The detection limit from pyrene/MBA mixture is down to 1 ppb on the μDADs, and only 2 ppm on the normal diatomite chromatography plate (Fig. S5). The experimental results demonstrate more than 1000 times improvement of the detection sensitivity using the μDADs compared to normal diatomite chromatography plates. We attribute this dramatic improvement to the strong micro-channel confinement of the fluid flow, which prevents the lateral diffusion of the target molecules within the μDADs.

3.6. On-chip sensing of cocaine from biofluid

In the case of sensitive detection of cocaine, the current detection platforms are gas chromatography (GC) [46], high performance liquid chromatography (HPLC) and chromatography in tandem with mass spectrometry (MS) [47,48]. Although the chromatography and mass spectrometry are accurate and reliable, they are expensive, time-consuming and require skilled personnel. Although accurate lab analysis techniques are available, instant, cost-effective and ease-of-use methods for on-site testing of cocaine from biofluid such as saliva, plasma and urine are yet to be developed for forensics and medical diagnosis. Here, μDADs were employed for on-chip detection of cocaine from human plasma. Cyclohexane and ethanol (v/v = 6:1) were used as the eluent for the separation of cocaine from plasma. In our experiment, cocaine was intentionally added into human plasma to obtain different concentrations (10 ppb–100 ppm). The macromolecules such as albumin and enzymes in plasma cannot diffuse on the μDADs due to the high molecular weight. Good separation and detection of cocaine is achieved using μDADs. The SERS spectra were shown in Fig. 5. The Raman peak at 1008 cm^{-1} was assigned to the aromatic ring breathing of cocaine. As shown in Fig. 5(a), the characteristic band of the cocaine exhibited a monotonous decrease in intensity following the decrease of the cocaine concentration in plasma. The detection limit for cocaine in plasma, which is defined as the signal-to-noise (SNR) ratio of 3 as marked by the blue line in Fig. 5(b), was 10 ppb using the μDADs. As a comparison, Brunetto et al. have developed column-switching LC method for cocaine detection, in which the LOD could achieved 80 ppb [49]. The 10 ppb LOD from μDADs is even better than that from the aforementioned LC laboratory analysis method. According to the report by National Highway Traffic Safety Administration [50], smoking 50 mg of cocaine would result in peak cocaine concentration in plasma at 230 ppb after 45 min, and the half-life-time for cocaine is approximately one hour. Therefore, our μDADs is sensitive enough to monitor cocaine from blood serum five hours after cocaine abusing.

4. Conclusions

In this pilot study, we have developed a new type of microfluidic devices, μDADs, for ultra-sensitive, label-free, ease-of-use and rapid sensing of illicit drugs from complex biofluidic samples. The μDADs are fabricated via a simple method by spin-coating and tape-stripping diatomite on glass. The μDADs can simultaneously separate small molecules from the complex background and acquire the SERS spectra of the target chemicals with high specificity after the deposition of plasmonic nanoparticles. Furthermore, the μDADs exhibit extremely high confinement of the analyte due to the ultra-small dimension of the diatomite microfluidic channels, which effectively increase the concentration of target molecules at the sensor surface. The experimental results achieved ultra-high detection sensitivity down to 1 ppb, which represents an improvement factor of more than 1000 times when compared to the normal chromatography plate device. To demonstrate the significant engineering potentials for forensic sensing, we have achieved ultra-sensitive detection of cocaine in human plasma with LOD of 10 ppb, which is even better than many laboratory analytical methods such as HP-LC and GC–MS. Such facile μDADs using hybrid plasmonic-diatomite biosilica, as a new type of cost-effective and ultra-sensitive microfluidic devices with multiplex sensing capabilities, will play a pivotal role in chemical and biological sensing, especially for POC drug screening.

Acknowledgements

The authors would like to acknowledge the support from the National Institutes of Health under Grant No. 1R21DA0437131, the National Science Foundation under Grant No. 1701329, the Unites States Department of Agriculture under Grant No. 2017-67021-26606, and talent scientific research fund of LSHU (No. 2017XJJ-037).

Appendix A. Supplementary data

Supplementary data associated with this article can be found, in the online version, at https://doi.org/10.1016/j.snb.2017.12.038.

References

[1] C. Yu, M.H. Davey, F. Svec, J.M. Fréchet, Monolithic porous polymer for on-chip solid-phase extraction and preconcentration prepared by photoinitiated in situ polymerization within a microfluidic device, Anal. Chem. 73 (2001) 5088–5096.
[2] M. Vázquez, B. Paull, Review on recent and advanced applications of monoliths and related porous polymer gels in micro-fluidic devices, Anal. Chim. Acta 668 (2010) 100–113.
[3] X. Li, D.R. Ballerini, W. Shen, A perspective on paper-based microfluidics: current status and future trends, Biomicrofluidics 6 (2012) 011301.
[4] E. Fu, C. Downs, Progress in the development and integration of fluid flow control tools in paper microfluidics, Lab Chip 17 (2017) 614–628.
[5] A.W. Martinez, S.T. Phillips, G.M. Whitesides, E. Carrilho, Diagnostics for the developing world: microfluidic paper-based analytical devices, Anal. Chem. 82 (2010) 3–10.
[6] A.W. Martinez, S.T. Phillips, M.J. Butte, G.M. Whitesides, Patterned paper as a platform for inexpensive, low-volume, portable bioassays, Angew. Chem. Int. Ed. 46 (2007) 1318–1320.
[7] Y. Lu, W. Shi, L. Jiang, J. Qin, B. Lin, Rapid prototyping of paper-based microfluidics with wax for low-cost, portable bioassay, Electrophoresis 30 (2009) 1497–1500.
[8] E. Carrilho, A.W. Martinez, G.M. Whitesides, Understanding wax printing: a simple micropatterning process for paper-based microfluidics, Anal. Chem. 81 (2009) 7091–7095.
[9] A.W. Martinez, S.T. Phillips, E. Carrilho, S.W. Thomas III, H. Sindi, G.M. Whitesides, Simple telemedicine for developing regions: camera phones and paper-based microfluidic devices for real-time, off-site diagnosis, Anal. Chem. 80 (2008) 3699–3707.
[10] Z. Nie, F. Deiss, X. Liu, O. Akbulut, G.M. Whitesides, Integration of paper-based microfluidic devices with commercial electrochemical readers, Lab Chip 10 (2010) 3163–3169.
[11] Z. Nie, C.A. Nijhuis, J. Gong, X. Chen, A. Kumachev, A.W. Martinez, et al., Electrochemical sensing in paper-based microfluidic devices, Lab Chip 10 (2010) 477–483.
[12] C.M. Cheng, A.W. Martinez, J. Gong, C.R. Mace, S.T. Phillips, E. Carrilho, et al., paper-based elisa, Angew. Chem. Int. Ed. 49 (2010) 4771–4774.
[13] W.Y. Wei, I.M. White, Chromatographic separation and detection of target analytes from complex samples using inkjet printed SERS substrates, Analyst 138 (2013) 3679–3686.
[14] C. Xu, Y. Liu, F. Su, A. Liu, H. Qiu, Nanoporous PtAg and PtCu alloys with hollow ligaments for enhanced electrocatalysis and glucose biosensing, Biosens. Bioelectron. 27 (2011) 160–166.
[15] W. Shan, T. Yu, B. Wang, J. Hu, Y. Zhang, X. Wang, et al., Magnetically separable nanozeolites: promising candidates for bio-applications, Chem. Mater. 18 (2006) 3169–3172.
[16] J.H. Moon, W. McDaniel, L.F. Hancock, Facile fabrication of poly (p-phenylene ethynylene)/colloidal silica composite for nucleic acid detection, J. Colloid Interface Sci. 300 (2006) 117–122.
[17] H. Yang, Y. Zhu, Size dependence of SiO 2 particles enhanced glucose biosensor, Talanta 68 (2006) 569–574.
[18] B.G. Trewyn, S. Giri, I.I. Slowing, V.S.-Y. Lin, Mesoporous silica nanoparticle based controlled release, drug delivery, and biosensor systems, Chem. Commun. (2007) 3236–3245.
[19] W. Yang, P.J. Lopez, G. Rosengarten, Diatoms: self assembled silica nanostructures, and templates for bio/chemical sensors and biomimetic membranes, Analyst 136 (2011) 42–53.
[20] D. Losic, G. Rosengarten, J.G. Mitchell, N.H. Voelcker, Pore architecture of diatom frustules: potential nanostructured membranes for molecular and particle separations, J. Nanosci. Nanotechnol. 6 (2006) 982–989.
[21] S. Leonardo, B. Prieto-Simón, M. Campàs, Past, present and future of diatoms in biosensing, TrAC Trends Anal. Chem. 79 (2016) 276–285.
[22] L. Zhen, N. Ford, D.K. Gale, G. Roesijadi, G.L. Rorrer, Photoluminescence detection of 2, 4, 6-trinitrotoluene (TNT) binding on diatom frustule biosilica functionalized with an anti-TNT monoclonal antibody fragment, Biosens. Bioelectron. 79 (2016) 742–748.
[23] L. De Stefano, L. Rotiroti, M. De Stefano, A. Lamberti, S. Lettieri, A. Setaro, et al., Marine diatoms as optical biosensors, Biosens. Bioelectron. 24 (2009) 1580–1584.
[24] C. Liu, Z. Wang, E. Li, Z. Liang, S. Chakravarty, X. Xu, et al., Electrokinetic manipulation integrated plasmonic–photonic hybrid raman nanosensors with dually enhanced sensitivity, ACS Sens. 2 (2017) 346–353.
[25] Y. Chen, G. Kang, A. Shah, V. Pale, Y. Tian, Z. Sun, et al., Improved SERS intensity from silver-coated black silicon by tuning surface plasmons, Adv. Mater. Interfaces 1 (2014).
[26] X. Kong, Y. Xi, P. LeDuff, E. Li, Y. Liu, L.-J. Cheng, et al., Optofluidic sensing from inkjet-printed droplets: the enormous enhancement by evaporation-induced spontaneous flow on photonic crystal biosilica, Nanoscale 8 (2016) 17285–17294.
[27] X. Kong, Y. Xi, P. Le Duff, X. Chong, E. Li, F. Ren, et al., Detecting explosive molecules from nanoliter solution: a new paradigm of SERS sensing on hydrophilic photonic crystal biosilica, Biosens. Bioelectron. 88 (2017) 63–70.
[28] H. Chu, D. Cao, B. Dong, Z. Qiang, Bio-diatomite dynamic membrane reactor for micro-polluted surface water treatment, Water Res. 44 (2010) 1573–1579.
[29] M. Al-Ghouti, M. Khraisheh, S. Allen, M. Ahmad, The removal of dyes from textile wastewater: a study of the physical characteristics and adsorption mechanisms of diatomaceous earth, J. Environ. Manage. 69 (2003) 229–238.
[30] M.S. Aw, S. Simovic, Y. Yu, J. Addai-Mensah, D. Losic, Porous silica microshells from diatoms as biocarrier for drug delivery applications, Powder Technol. 223 (2012) 52–58.
[31] R.A. Shawabkeh, M.F. Tutunji, Experimental study and modeling of basic dye sorption by diatomaceous clay, Appl. Clay Sci. 24 (2003) 111–120.
[32] H. Hadjar, B. Hamdi, M. Jaber, J. Brendlé, Z. Kessaissia, H. Balard, et al., Elaboration and characterisation of new mesoporous materials from diatomite and charcoal, Microporous Mesoporous Mater. 107 (2008) 219–226.
[33] W. Shen, M. Li, C. Ye, L. Jiang, Y. Song, Direct-writing colloidal photonic crystal microfluidic chips by inkjet printing for label-free protein detection, Lab Chip 12 (2012) 3089–3095.
[34] S. Zong, Z. Wang, H. Chen, J. Yang, Y. Cui, Surface enhanced Raman scattering traceable and glutathione responsive nanocarrier for the intracellular drug delivery, Anal. Chem. 85 (2013) 2223–2230.
[35] A. Dugay, C. Herrenknecht, M. Czok, F. Guyon, N. Pages, New procedure for selective extraction of polycyclic aromatic hydrocarbons in plants for gas chromatographic–mass spectrometric analysis, J. Chromatogr. A 958 (2002) 1–7.
[36] K.C. Grabar, R.G. Freeman, M.B. Hommer, M.J. Natan, Preparation and characterization of Au colloid monolayers, Anal. Chem. 67 (1995) 735–743.
[37] A.R. Guerrero, R.F. Aroca, Surface-enhanced fluorescence with shell-isolated nanoparticles (SHINEF), Angew. Chem. Int. Ed. 50 (2011) 665–668.
[38] L. De Stefano, P. Maddalena, L. Moretti, I. Rea, I. Rendina, E. De Tommasi, et al., Nano-biosilica from marine diatoms: a brand new material for photonic applications, Superlattices Microstruct. 46 (2009) 84–89.
[39] E. De Tommasi, I. Rea, V. Mocella, L. Moretti, M. De Stefano, I. Rendina, et al., Multi-wavelength study of light transmitted through a single marine centric diatom, Opt. Express 18 (2010) 12203–12212.
[40] M.B. Tennikov, N.V. Gazdina, T.B. Tennikova, F. Svec, Effect of porous structure of macroporous polymer supports on resolution in high-performance membrane chromatography of proteins, J. Chromatogr. A 798 (1998) 55–64.
[41] Y. Xie, X. Wang, X. Han, X. Xue, W. Ji, Z. Qi, et al., Sensing of polycyclic aromatic hydrocarbons with cyclodextrin inclusion complexes on silver nanoparticles by surface-enhanced Raman scattering, Analyst 135 (2010) 1389–1394.
[42] C.J. Orendorff, A. Gole, T.K. Sau, C.J. Murphy, Surface-enhanced Raman spectroscopy of self-assembled monolayers: sandwich architecture and nanoparticle shape dependence, Anal. Chem. 77 (2005) 3261–3266.
[43] C.V. Raman, K.S. Krishnan, A new type of secondary radiation, Nature 121 (1928) 501–502.
[44] D. Choi, T. Kang, H. Cho, Y. Choi, L.P. Lee, Additional amplifications of SERS via an optofluidic CD-based platform, Lab Chip 9 (2009) 239–243.
[45] X. Kong, E. Li, K. Squire, Y. Liu, B. Wu, L.J. Cheng, et al., Plasmonic nanoparticles-decorated diatomite biosilica: extending the horizon of on-chip chromatography and label-free biosensing, J. Biophotonics 10 (2017) 1473–1484.
[46] L.S. de Jager, A.R. Andrews, Development of a screening method for cocaine and cocaine metabolites in urine using solvent microextraction in conjunction with gas chromatography, J. Chromatogr. A 911 (2001) 97–105.
[47] I. Roy, T. Jefferies, M. Threadgill, G. Dewar, Analysis of cocaine, benzoylecgonine, ecgonine methyl ester, ethylcocaine and norcocaine in human urine using HPLC with post-column ion-pair extraction and fluorescence detection, J. Pharm. Biomed. Anal. 10 (1992) 943–948.
[48] M.E. Hows, L. Lacroix, C. Heidbreder, A.J. Organ, A.J. Shah, High-performance liquid chromatography/tandem mass spectrometric assay for the simultaneous measurement of dopamine, norepinephrine, 5-hydroxytryptamine and cocaine in biological samples, J. Neurosci. Methods 138 (2004) 123–132.
[49] M. Brunetto, Y.D. Cayama, L.G. García, M. Gallignani, M. Obando, Determination of cocaine and benzoylecgonine by direct injection of human urine into a column-switching liquid chromatography system with diode-array detection, J. Pharm. Biomed. Anal. 37 (2005) 115–120.
[50] N. Reddy, Y. Yang, Properties and potential applications of natural cellulose fibers from the bark of cotton stalks, Bioresour. Technol. 100 (2009) 3563–3569.

Biographies

Xianming Kong is an Associate Professor at the College of Chemistry, Chemical Engineering and Environment Engineering at Liaoning Shihua University, Fushun, P. R. China. He was a Postdoctoral Scholar at the School of Electrical Engineering and Computer Science at Oregon State University from 2015 to 2017. He received his PhD degree in Physical Chemistry from Nanjing University, Nanjing, China, in 2012. From 2012 to 2015, he worked as a postdoctoral researcher in the School of Chemical Technology, Aalto University, Finland. His current research work focuses on the development of surface-enhanced Raman scattering (SERS) sensors for chemical and biological sensing.

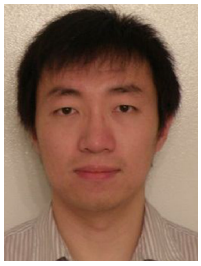

Xinyuan Chong received his Ph.D. degree from the School of Electrical Engineering and Computer Science at Oregon State University in 2017. He received his B.S. and M.S. in Physics from Tsinghua University in 2008 and 2011 respectively. His current research interests include plasmonic-enhanced optical sensor for chemical detection, gas sensing, and biomedical applications.

Kenny Squire is a PhD candidate in the School of Electrical Engineering and Computer Science at Oregon State University. He received his B.S. degree in Electrical Engineering from Brigham Young University in 2015. His research focuses on optical biosensors utilizing surface plasmon resonance and surface-enhanced Raman spectroscopy.

Alan X. Wang is an Associate Professor of the School of Electrical Engineering and Computer Science at Oregon State University since 2011. He received his Ph.D. degree in Electrical and Computer Engineering from the University of Texas at Austin in 2006. From 2007 to 2011, he was with Omega Optics, Inc., where he served as the Chief Research Scientist for 9 SBIR/STTR projects. His research interests include nanophotonic devices for optical interconnects, and optical sensors for chemical and biological detection. His current research activities are sponsored by the National Science Foundation, the National Institutes of Health, Oregon Nanoscience and Microtechnologies Institute, the National Energy Technology Laboratory, and industrial sponsors such as Hewlett-Packard. He has more than 70 journal publications and 70 conference presentations, and also holds three U.S. patents. He is a senior member of IEEE Photonics, SPIE and OSA.